



Coronavirus pandemic: An opportunity to study the anthropogenic impact on micro-climate conditions and CaCO₃ crystal morphology in the Nerja Cave (SE Spain)



C. Liñán^{a,b,*}, C. Jiménez de Cisneros^c, J. Benavente^d, I. Vadillo^a, Y. del Rosal^b, L. Ojeda^a

^a Centre of Hydrogeology of University of Malaga and Department of Ecology and Geology, Faculty of Science, University of Malaga, 29071 Malaga, Spain

^b Research Institute, Nerja Cave Foundation, Carretera de Maro, s/n, 29787 Nerja, Malaga, Spain

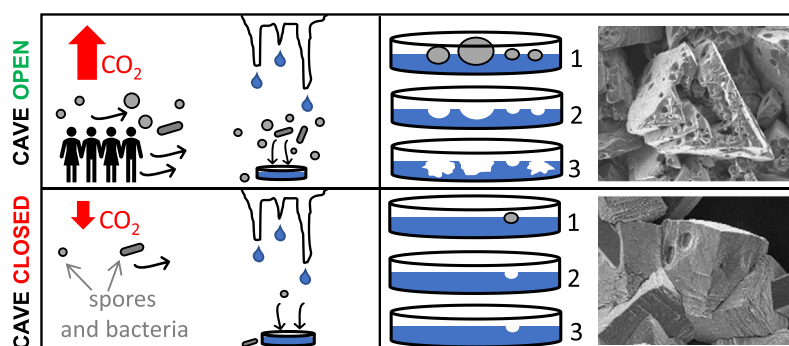
^c Instituto Andaluz de Ciencias de la Tierra (IACT-UGR), 18100 Armilla, Granada, Spain

^d Water Research Institute and Department of Geodynamics, University of Granada, 18071 Granada, Spain

HIGHLIGHTS

- Cave closure due to the pandemic (coronavirus) has allowed the study of its pristine conditions.
- Visitors, spores and bacteria condition the texture of carbonate precipitates.
- Some micro-cavities are induced by micro-organisms during crystal formation.
- Anthropogenic CO₂ enlarges micro-cavities of biotic origin.
- The isotopical signature of the soil and vadose air is constrained.

GRAPHICAL ABSTRACT



ARTICLE INFO

Editor: Daniel Alessi

Keywords:

Anthropogenic impact
Carbon dioxide
Carbonate precipitate
COVID-19
Micro-organism
Tourist cave

ABSTRACT

Following the declaration of the COVID-19 pandemic, the Spanish Government restricted non-essential movements of all citizens and closed all public spaces, such as the Nerja Cave, until May 31, 2020. This particular condition of the closure of the cave provided a unique opportunity to study the micro-climate conditions and carbonate precipitation in this tourist cave without the presence of visitors. Our results show the significant effect of visitors on the air isotopic signature of the cave and on the genesis of the extensive dissolution features affecting the carbonate crystals formed in the tourist sector of the cave, alerting us to the possible corrosion of the speleothems located there. The movement of visitors within the cave also favours the mobilisation of aerial fungi and bacterial spores and their subsequent sedimentation simultaneously with the abiotic precipitation of carbonates from the drip water. The traces of these biotic elements could be the origin of the micro-perforations previously described in the carbonate crystals formed in the tourist galleries of the cave, but they are subsequently enlarged due to abiotic dissolution of the carbonates through these weaker zones.

* Corresponding author at: Centre of Hydrogeology of University of Malaga, Department of Geology, Faculty of Science, University of Malaga, 29071 Malaga, Spain.

E-mail addresses: crilinbae@uma.es cbaena@cuevadenerja.es (C. Liñán), concepcion.cisneros@csic.es (C.J. de Cisneros), jbenaven@ugr.es (J. Benavente), vadillo@uma.es (I. Vadillo), yolanda@cuevadenerja.es (Y. del Rosal), luciaor@uma.es (L. Ojeda).

<http://dx.doi.org/10.1016/j.scitotenv.2023.163693>

Received 9 December 2022; Received in revised form 19 April 2023; Accepted 19 April 2023

Available online 24 April 2023

0048-9697/© 2023 The Authors. Published by Elsevier B.V. This is an open access article under the CC BY-NC-ND license (<http://creativecommons.org/licenses/by-nc-nd/4.0/>).

1. Introduction

On 11 March 2020, the World Health Organization (WHO) classified COVID-19 as a pandemic. Three days later (14 March), the Spanish Government decreed a state of alarm, which limited the non-essential movements of all citizens and closed spaces for public use, such as schools, universities, parks, theatres, gyms, restaurants and tourist sites. These measures aimed to protect the citizens' health, contain the progression of the COVID-19 disease, and strengthen the public health system. On 28 April the Spanish Government approved a de-escalation plan for the transition towards a “New Normality”, which was gradually implemented up to 21 June, when the state of alarm ended. During this de-escalation plan, restaurants, hotels, museums, and other tourist sites were re-opened progressively depending on the evolution of the pandemic in each province, although with restrictions (mobility or capacity, for example). In Andalusia (S Spain), the tourist sites (monuments, museums, tourist caves) mainly reopened in June 2020. Thus, the lockdown of Spanish citizens in their homes to avoid the spread of the epidemic, generated unique conditions in the tourist sites, due to being free of anthropogenic impact for approximately two and a half months.

The Nerja Cave is one of the most important heritage tourist caves in Spain, with about 450,000 visitors per year and more than 500 prehistoric graphic manifestations (Sanchidrián et al., 2017). This high number of visitors increases air temperature, relative humidity and, particularly, carbon dioxide concentration within the cave (Carrasco et al., 2002). However, other natural factors such as the rate and modes of natural ventilation (Liñán et al., 2018, 2020) or the seasonal fluctuations of the CO₂ content in the soil or drip-water flow also influence the micro-climate cave parameters.

Carbon dioxide gas is also a key component in the dissolution and precipitation of carbonates in karstic systems (White, 1988, 1997; Dragovich and Grose, 1990; Dreybrodt, 2000; Dreybrodt and Eisenlohr, 2000) and thus, a critical parameter in the conservation of speleothems and subterranean rock paintings (Fernández et al., 1986; Hoyos et al., 1998; Sánchez-Moral et al., 1999; Houillon et al., 2017). Infiltrating water, moving from the surface to the caves, continuously interacts with the gaseous and solid phases of the soil zone first and the vadose zone later. The percolating water increases the CO₂ levels and dissolves the carbonate [(CO₃)₂CaMg] on its way down. When the vadose water enters the cave, this CO₂-saturated water can degas from the solution if the pCO₂ of the cave air is lower than the pCO₂ of the vadose water. This process drives the carbonate precipitation and the formation of speleothems within the caves. However, the chemical reaction (Eq. (1)) is reversible, so the rate of carbonate precipitation (or dissolution) is highly affected by changes in the amount and chemistry of the dripping water and also by fluctuations of the CO₂ levels of the cave atmosphere:



On the other hand, micro-organisms can cause microbiologically induced carbonate precipitation (MICP), a natural process mediated mainly by bacteria (Koning et al., 2022). Furthermore, CO₂ and water released by bacteria as a byproduct of their metabolic activity and present in the environment may influence the dissolution/precipitation processes by shifting the chemical reaction (Eq. (1)) in one way or the other. For instance, in the Altamira Cave (Spain), Cuezva et al. (2012) reported that areas heavily colonised by bacteria, with visible biomineralization processes, were able to capture atmospheric CO₂, causing a decrease in the pH and subsequent dissolution of the host rock (limestone). The release of Ca²⁺ in the solution around bacteria can result in mineral precipitation in lower humidity and/or CO₂ periods.

Previous studies about the carbonate precipitates formed in the cave (Jiménez de Cisneros et al., 2020; Jurado et al., 2022) showed clear differences between those obtained in the tourist and non-tourist chambers. The former showed the presence of micro-organisms and highly altered crystals, while the latter exhibited well-formed crystals with few traces of dissolution. Although the presence of people in the caves can induce changes in

their microbiological conditions, both as a consequence of human metabolism and the dispersion of nutrients and micro-organisms in the caves (Mulec, 2014; Mulec et al., 2017), the visitors' role in the differences observed in mineral precipitates in the visitable sector compared to those formed in the non-visitable sector of the cave is not entirely clear.

The closure of the cave to the public due to the pandemic provided the opportunity to obtain micro-climate data and mineral precipitates from the tourist sector but without the presence of visitors. This has allowed us to compare the micro-climate data series recorded in the cave and the textural and mineralogical characteristics of the carbonate precipitates formed in the tourist galleries during two periods: (1) the pre-pandemic period, with a regular regime of visits and (2) the pandemic period (from 11 March to December 2020) that included one closure period of the cave: from 13 March to 31 May (80 days). Our results have allowed us to determine the impact of visitors and micro-organisms on the current carbonate precipitation and their textures, as well as to advance our knowledge of the natural processes that affect air composition in the cave. Amongst them, we highlight the “vadose air” contribution as a significant source of cave air CO₂ during some periods, which has been partially masked until now by the daily presence of visitors.

2. Site description

The Nerja Cave (NC, Fig. 1) is located in the south of the Iberian Peninsula (Malaga province, Andalusia Region), in an area of great environmental value, between two protected natural sites. The cavity covers an area of 35,000 m² and its development is practically horizontal, situated between 123 and 191 m above sea level (m a.s.l.). About a third of the cave, the so-called Tourist Galleries, has been open for visitors since 1960, a year after its discovery. The rock thickness above the cave varies from 4 to 50 m in the area opened to tourism, exceeding 80 m in the non-visitable area of the cave, according to the elevation of the topographic surface.

The cave development occurs in the unsaturated zone of the Sierra Almijara carbonate aquifer, made up of highly fractured Triassic dolomitic marbles (Andreo et al., 2018), with soil cover rarely exceeding thicknesses of 15 cm. The climate in the study area is coastal Mediterranean, with average annual precipitation slightly below 500 mm/year and a mean annual temperature of 18.5 °C (Liñán et al., 2007). Rainfall and, in the case of the chambers located below the gardens, water for irrigation also infiltrates through fissures and fractures in the marble and drip water from the cave roof. Within the cave, two main types of drip water have been identified: one sampled in the chambers closest to the entrance and the other in the rest of the cavity. Besides the general meteoric origin, in the first type there is also water coming from a nearby borehole used for irrigation. Drip water is supersaturated with calcite and produces calcium carbonate precipitates.

The cave is open throughout the whole year except for two days (1 January and 15 May). The monthly distribution of visitors is similar to previous years, with a minimum in January–February and November–December, ranging between 9000 and 33,000 visitors/month, with a maximum in August, with 83,000–119,000 visitors/month (Carrasco et al., 2002). At present, there is a limited number of 350 visitors/h permitted in July and August with 9 h of daily opening, and 250 visitors/h during the rest of the year, with 6 h of daily opening. The anthropogenic impact is reflected in daily increases in temperature, relative humidity and air CO₂ concentration during the opening hours and a decrease during closure (Carrasco et al., 2002), amongst other effects.

In the Nerja Cave, four ventilation regimes (*winter*, *spring*, *summer* and *autumn*) and two ventilation modes with opposite airflow directions (UAF- and DAF- modes) have been defined during the annual cycle (Liñán et al., 2018, 2020). During the *winter* regime (from October/early November to April/mid-May), maximum ventilation exists and the airflow directions are normally from the lowest entrances of the cave (E1-E2-E3) to the highest voids of the karst system (joints, fractures). This type of ventilation is the so-called UAF-mode (upward airflow) and is activated when the temperature (T) of the external air is lower than the cave air (T_{ext} < T_{int}).

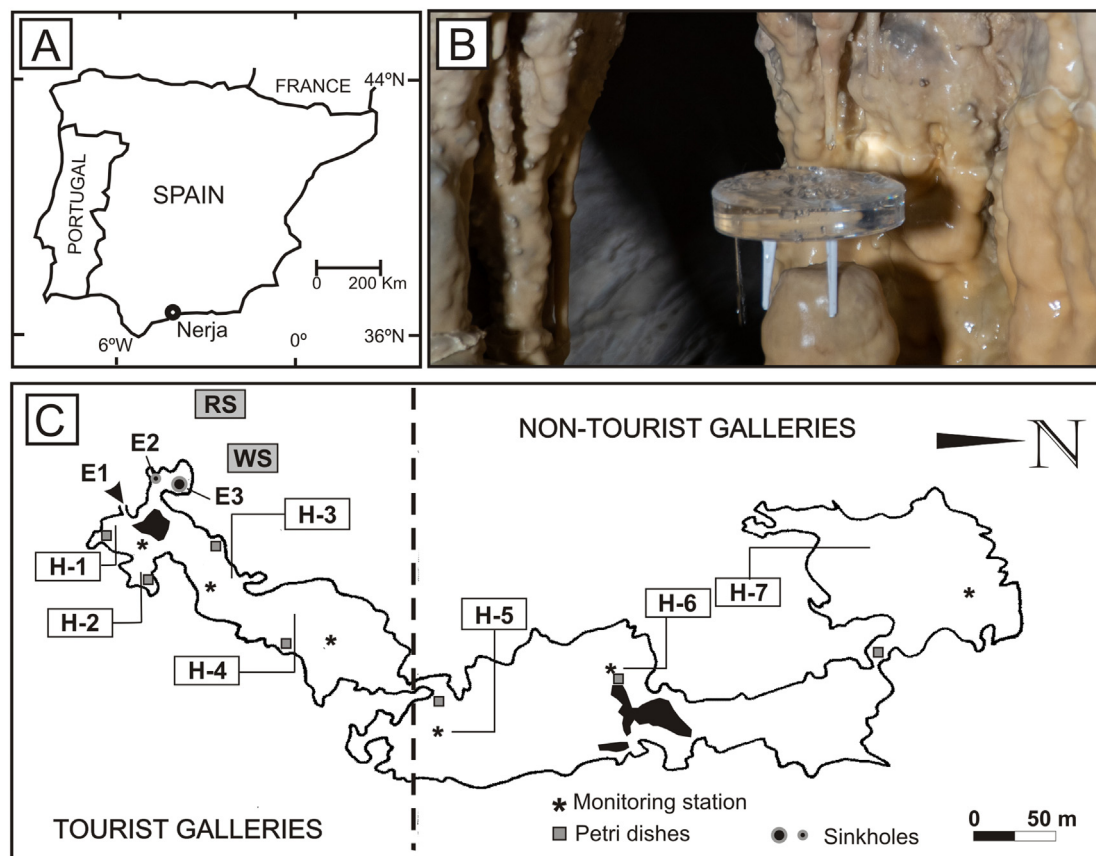


Fig. 1. (A) Geographical location of the Nerja Cave, (B) image of one of the Petri dishes and (C) map of the Nerja Cave, with the location of the monitoring stations, carbonate precipitation on Petri dishes, weather station (WS), borehole research site (RS) and the different galleries of the Nerja Cave (H-1 to H-7). E1: tourist entrance, E2 and E3: sinkholes. Points WS and RS are outside the cave, and their location is approximate.

During the *summer* regime (from mid-June/July to early September), the ventilation is the lowest of the annual cycle and a reversed airflow pattern exists: the cave air is expelled through the lowest entrances and external air is sucked in through the highest entrances. This so-called *DAF*-mode ventilation (downward airflow) is activated when ΔT ($T_{\text{ext}} - T_{\text{int}}$) is higher than 5°C . The transitional ventilation regimes —*spring* (from April/mid-May to early June) and *autumn* (from early September/October to early November)— are the most complex, with changing airflow directions of a diurnal or poly-diurnal periodicity.

Since the cave opened in 1960, it has only twice been closed to the public for several days in a row: (a) in December 1996 (9 days; from 16 to 24 December), when a group of tenant farmers squatted in the cave due to a social conflict between them and the owner of the farmlands; and (b) in 2020, due to the COVID-19 pandemic (80 days: from 13 March to 31 May; and 38 days from 10 November to 17 December).

3. Material and methods

The Nerja Cave has a network of monitoring stations located longitudinally (Fig. 1C) consisting of data-loggers CR1000 (Campbell Scientific) with special sensors selected for the range of measurements expected and periodically calibrated by the manufacturer. The stations record hourly air temperature, relative humidity (RH), CO_2 concentration, atmospheric pressure, air speed, and airflow direction, amongst other parameters. Cave air CO_2 concentrations are measured using an infrared absorption sensor model GMM222-Vaisala (measuring range 0–5000 ppmv, accuracy $\pm 1.5\%$). Air temperature and relative humidity are measured by a humidity and temperature probe model HMP155A- Vaisala (measuring range 0–100 % RH, accuracy $\pm 1.0\%$; measuring range -80 to $+60^\circ\text{C}$, accuracy $\pm 0.17^\circ\text{C}$). Air speed and airflow direction are measured by an

ultrasonic wind sensor WindSonic (measuring range: 0–60 m/s, accuracy $\pm 2\%$; $0-359^\circ$, $\pm 2^\circ$). The pressure is measured by a barometer model PTB 110-Vaisala (measuring range: 500–1100 hPa, accuracy ± 0.3 hPa). Since September 2017, a Picarro G2201-i Cavity Ring-Down Spectrometer measures the CO_2 and CH_4 air concentrations and the C isotope relation ($\delta^{13}\text{C}-\text{CO}_2$ and $\delta^{13}\text{C}-\text{CH}_4$) in real-time and in situ in some halls (Ojeda et al., 2018). In this study, we analysed the air CO_2 (concentration and isotopic composition) measured by the spectrometer in the H-3 chamber. The CO_2 measuring range of the spectrometer is 100–4000 ppmv; accuracy: 200 ppb + 0.05 % of reading (^{12}C), 10 ppb + 0.05 % of reading (^{13}C).

A weather station (169 m a.s.l.) belonging to the State Agency of Meteorology (AEMET), located few metres from the Nerja Cave (WS in Fig. 1), records the external atmospheric parameters hourly: temperature and relative humidity of the air, atmospheric pressure, evaporation and velocity and direction of the wind, amongst others (Liñán et al., 2007).

In order to evaluate the growth dynamics of the current speleothems and its relationship with the environmental parameters of the cave, in 2017, several Petri dishes were placed in different chambers of the cave (Fig. 1B, C) below active drip water points during part of the year or all year round. In the external chambers (H-1 to H-3), the drip water comes from rainwater infiltration and irrigation of the gardens above. In the rest of the cavity (chambers H-4 to H-7), the drip water is exclusively of meteoric origin. After being exposed to drip water for a variable time, the obtained precipitates in Petri dishes were sampled for mineralogical, isotopic, and microscopic analysis. On 21 April 2020 two of the Petri dishes (H-3 and H-4 sites) were substituted to obtain new mineral precipitates during the closure period, without any visitors in the cave. In this study, we analysed the mineral precipitates from Petri dishes obtained during the *pre-pandemic period* (from December 2017 to June 2018 and from June to

September 2018, H-1 to H-7 sites) and the *pandemic period* (closed to the public, 21 April to 31 May 2020, H-3 and H-4 sites).

For the microscopic observations of the current precipitates, a high-resolution scanning electron microscope HRSEM (AURIGA from Carl Zeiss SMT) was used, after specific preparations made in the laboratory of the Centre for Scientific Instrumentation (CIC, University of Granada).

Periodically (usually weekly or fortnightly), the pH and the electrical conductivity (EC) of the drip points associated with the Petri dishes were measured in situ using calibrated HORIBA portable equipment. The pH was measured using the LAQUAtwin-pH -11 model pH meter (resolution: 0.1 pH, accuracy: ± 0.1 pH); EC was measured with the LAQUAtwin-B771 model EC meter (resolution: 1 $\mu\text{S}/\text{cm}$ for conductivity range 9–2000 $\mu\text{S}/\text{cm}$, accuracy $\pm 2\%$). The drip water flow rate was measured by counting the number of drops which had fallen in 2 min.

The Keeling plot method was used to determine the carbon isotope composition of CO_2 entering the Nerja Cave. Cave air CO_2 composition is a function of the CO_2 inputs from different sources, i.e., outside atmospheric air, human exhalation (visitors' breath), vadose CO_2 , soil CO_2 , etc. This mixing process between the outside atmosphere and a CO_2 -rich source is often characterized by two end-members which identify each contribution on the cave air composition by using a mass and isotope balance approach, the Keeling method (Keeling, 1958; Pataki et al., 2003):

$$\delta^{13}\text{C}_{\text{cave}} = \text{CO}_{2\text{ atm}} \left(\delta^{13}\text{C}_{\text{atm}} - \delta^{13}\text{C}_{\text{source}} \right) \frac{1}{\text{CO}_{2\text{ cave}}} + \delta^{13}\text{C}_{\text{source}} \quad (1)$$

where $\delta^{13}\text{C}_{\text{cave}}$ and $\text{CO}_{2\text{ cave}}$ are the isotopic value and concentration of the cave air sample, respectively, $\delta^{13}\text{C}_{\text{atm}}$, and $\text{CO}_{2\text{ atm}}$ are the isotopic value and concentration of the atmosphere, and $\delta^{13}\text{C}_{\text{source}}$ is the isotopic value of the CO_2 produced in the surrounding epikarst (vadose and/or soil air) and/or human respiration. Eq. 2 was fitted to the data using least squares regression for the points H-3 and H-6, and for each of the four subdivisions carried out in the study period, according to the criteria that will be explained later on.

4. Results

4.1. Micro-climate parameters

Fig. 2 shows the daily evolution of the cave air temperature, relative humidity and CO_2 concentration in the H-3 chamber during 2019 and 2020. We selected this chamber because of its intermediate location in the tourist sector of the cavity. The daily number of visitors and ΔT ($T_{\text{ext}} - T_{\text{int}}$; external and cave air temperature differences) are also represented.

In 2019 the annual evolution of all the parameters was similar to those reported and described for the cave in previous years (Carrasco et al., 2002; Jiménez de Cisneros et al., 2020), with a maximum number of visitors, air temperature, relative humidity and cave air CO_2 concentrations in summer (from June/July to September/October) and minimum values in winter (from November to February/March). The values registered for air temperature and relative humidity and their temporal evolution are relatively similar for 2019 and 2020 (Fig. 2A, B). During the two periods in which the cave was closed to the public (from 13 March to 31 May and from 10 November to 17 December), the cave air CO_2 concentrations were clearly lower than in 2019 (Fig. 2C). The seasonal evolution for cave air CO_2 concentration is different too, with minimum values during the two closure periods of the cave and maximum values in summer. In 2020, the number of visitors was lower than in 2019, except from January to mid-March. However, the temporal evolution of the number of visitors is similar for both years except during the closure periods of the cave to the public (Fig. 2D). The ΔT , which determines the natural cave ventilation degree, was also similar for both years (Fig. 2E).

Fig. 3 shows the hourly evolution for the number of visitors and the main environmental parameters in Nerja Cave (H-3 chamber, red lines) and external air (black lines) from 1 March to 30 June 2020. Three periods (a, b, c) are differentiated depending on the number of visitors which were

closely linked to the evolution of the pandemic. During period a (from 1 to 12 March 2020), the number of visitors (10,250) was less than in 2019 (12,114 visitors) due to the limited mobility of tourists given the worldwide advance of COVID-19. Period b (from 13 March to 31 May 2020) corresponds to the first closure period of the pandemic (0 visitors; 105,396 visitors in 2019) and is delimited in Fig. 3 by the vertical dashed black lines. During period c (June 2020), some 3723 visitors entered the cave, a value equivalent to 9 % of the visitors in June 2019 (41,957 visitors).

In each of the periods b and c, we distinguish two sub-periods (\mathbf{b}_w , \mathbf{b}_{sp}) and (\mathbf{c}_{sp} , \mathbf{c}_{su}) depending on the cave ventilation regime: *winter* (\mathbf{b}_w , from 13 March to 30 April), *spring* (\mathbf{b}_{sp} , from 1 to 31 May; \mathbf{c}_{sp} , from 1 to 14 June) and *summer* (\mathbf{c}_{su} , from 14 to 30 June).

4.1.1. Pre-pandemic period. Cave open, regular regime of visits

During period a (pre-pandemic), the cave air temperature and relative humidity follow approximately the same pattern as the external air (Fig. 3C, D), with some differences in the case of the air relative humidity during the DAF-mode ventilation. The natural variations induced by the outside air are added to the anthropogenic variations caused by the presence of visitors in the cave and by the use of electric lighting. They mainly produce daily increases in the air temperature and CO_2 concentration of the tourist galleries during opening hours and decreases during closing. The daily increases of the parameters from the baseline of each day are between 0.19 °C and 0.36 °C (air temperature) and between 119 and 358 ppmv (air CO_2) depending on the number of visitors. The mean value of each parameter defines the baseline of each day during the hours when the cave is closed to public. The air CO_2 concentrations in the H-3 chamber (daily mean values, Fig. 4A) ranged from 515 to 676 ppmv, with a mean value of 568 ppmv. The isotopic signature ranged from -14.4% to -11.8% , with a mean value of -12.8% . During this period, both parameters show opposite evolutions: ascending in the case of the isotopic signal and descending in the case of the air CO_2 concentration.

Cave air CO_2 composition is a function of the CO_2 inputs from different sources and ventilation. This mixing process between a CO_2 -rich source and the external air is often characterized by two end-members that identify each cave air composition contribution using the Keeling plot method (Keeling, 1958). In the Nerja Cave, the two end-members would be the atmospheric air and a light-member with depleted $\delta^{13}\text{C}_{\text{CO}_2}$ values identified as vadose air (Ojeda et al., 2019). Considering for the external air the same isotopic and concentration values (-8.9% and 400 ppmv, respectively) for all studied periods, the source of CO_2 entering Nerja Cave in period a (winter, cave open) had an isotopic signature of -22.4% for H-3 hall (Fig. 5A) (CI -22.5 to -22.2% ; CI: Confidence Interval) and of -22.2% for H-6 hall (Fig. 5B) (CI -22.6 to -21.7%).

4.1.2. Pandemic period. Cave closed, no visitors

During period b (closure period, 0 visitors), the daily mean values of CO_2 range from 422 to 457 ppmv, with a mean value of 434 ppmv. While in the period with a regular regime of visits (period a) the daily increases in air temperature and CO_2 were observed, in period b those were not recorded (Fig. 3B, C). In turn, in period b the air CO_2 concentration gradually reduces until it reaches values close to atmospheric values (Fig. 3B). The isotopic signal of CO_2 (Fig. 4A) range from -11.0% to -9.2% (mean value of -9.9%) and shows a general downward trend, which is more pronounced from 22 April onwards as ΔT values decrease and become positive (Fig. 4B). Although the air CO_2 concentration is relatively constant in this period, during the times in which ΔT values are positive it increases slightly while its isotopic signal becomes lighter (see arrows in Fig. 4A). The light source of CO_2 entering Nerja Cave in period \mathbf{b}_w (cave closed, winter regime; Fig. 4A) has an isotopic signature of -18.0% for the H-3 chamber (Fig. 5C) (CI -19.3 to -16.6%) and of -23.2% for the H-6 chamber (Fig. 5D) (CI -24.56 to -21.9%). In period \mathbf{b}_{sp} (cave closed, spring regime), the isotopic signature of the source of CO_2 entering the cave was -25.9% for H-3 hall (Fig. 5E) (CI -26.3 to -25.5%) and of -27.1% for H-6 hall (Fig. 5F) (CI -27.6 to -26.6%).

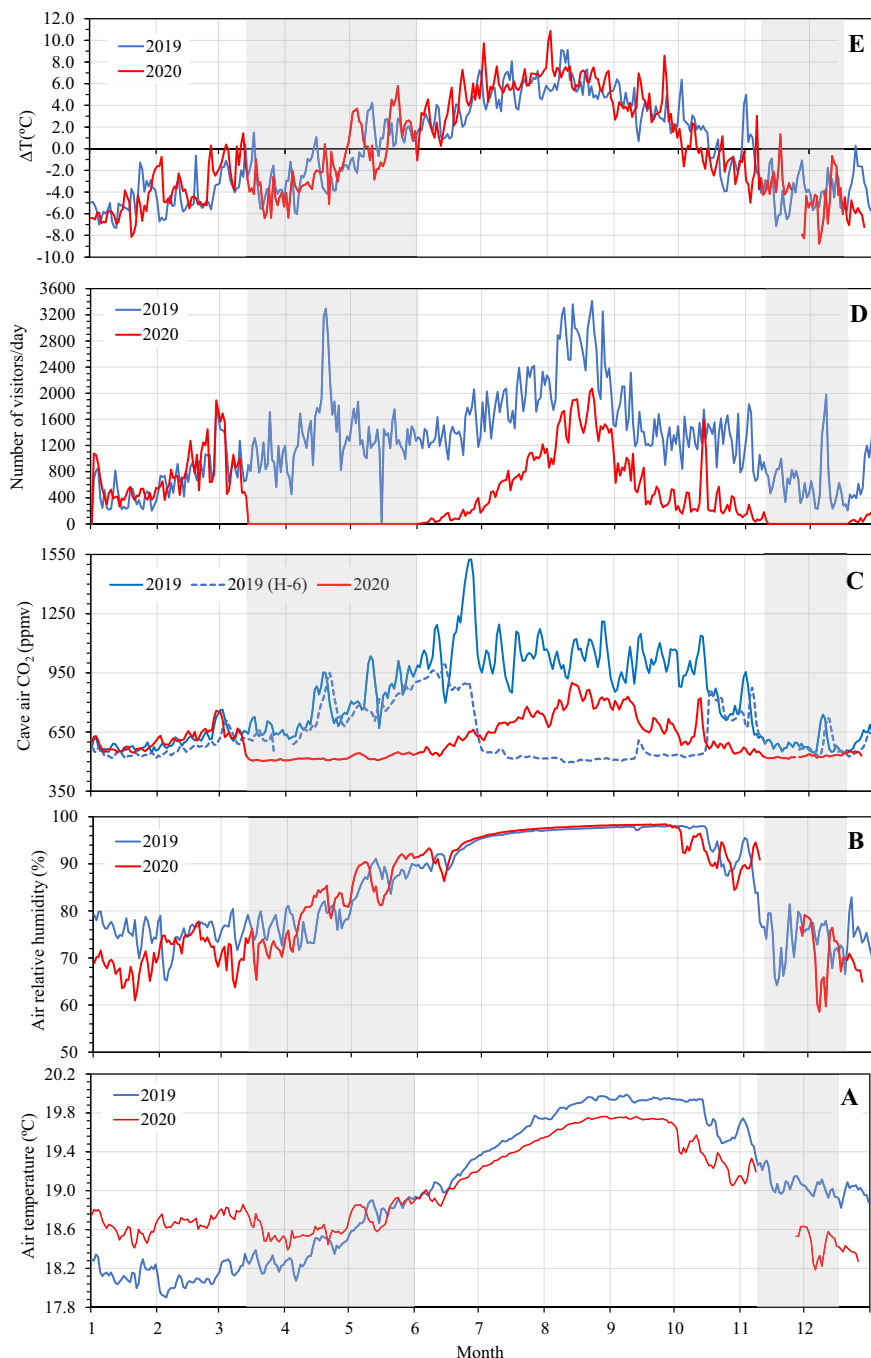


Fig. 2. Annual evolution of the air temperature (A), relative humidity (B), cave air CO₂ concentration (C), daily visitors (D) and external-internal air temperature differences (E) registered in H-3 hall during 2019 (blue lines) and 2020 (red lines). Dotted line in graph C: air CO₂ concentration in H-6 hall (non-tourist sector). Grey bars: cave closed to the public.

4.1.3. Pandemic period. Reopening of the cave to the public

During period c (June, reopening of the cave to the public), the daily anthropogenic increases observed in air temperature and CO₂ reappear, especially when the number of daily visitors is up by 200 people. The air CO₂ concentration increases progressively from about 440 to 540 ppm (Figs. 3B and 4A) and its isotopic signal becomes lighter, with values between -13.0‰ and -10.3‰ , and a mean value of -11.5‰ . In this period, the CO₂ source entering the cave had an isotopic signature of -23.9‰ for H-3 hall (Fig. 5G) (CI -24.1 to -23.7‰) and of -24.4‰ for H-6 hall (Fig. 5H) (CI -24.6 to -24.1‰).

4.2. Carbonate precipitation and drip waters

Fig. 6 shows the high-resolution scanning electron microscopy photographs of the carbonate precipitates obtained in several cave chambers for different periods: (1) winter ventilation period with normal visitability (December 2017–June 2018, 7 months), (2) summer period with normal visitability (from June to September 2018, 4 months) and (3) closure period of the cave (from 21 April to 31 May 2020; 1 month). When the cave is open to the public, the precipitates collected in the tourist sector are formed mainly from calcite crystals with rounded and irregular faces and abundant

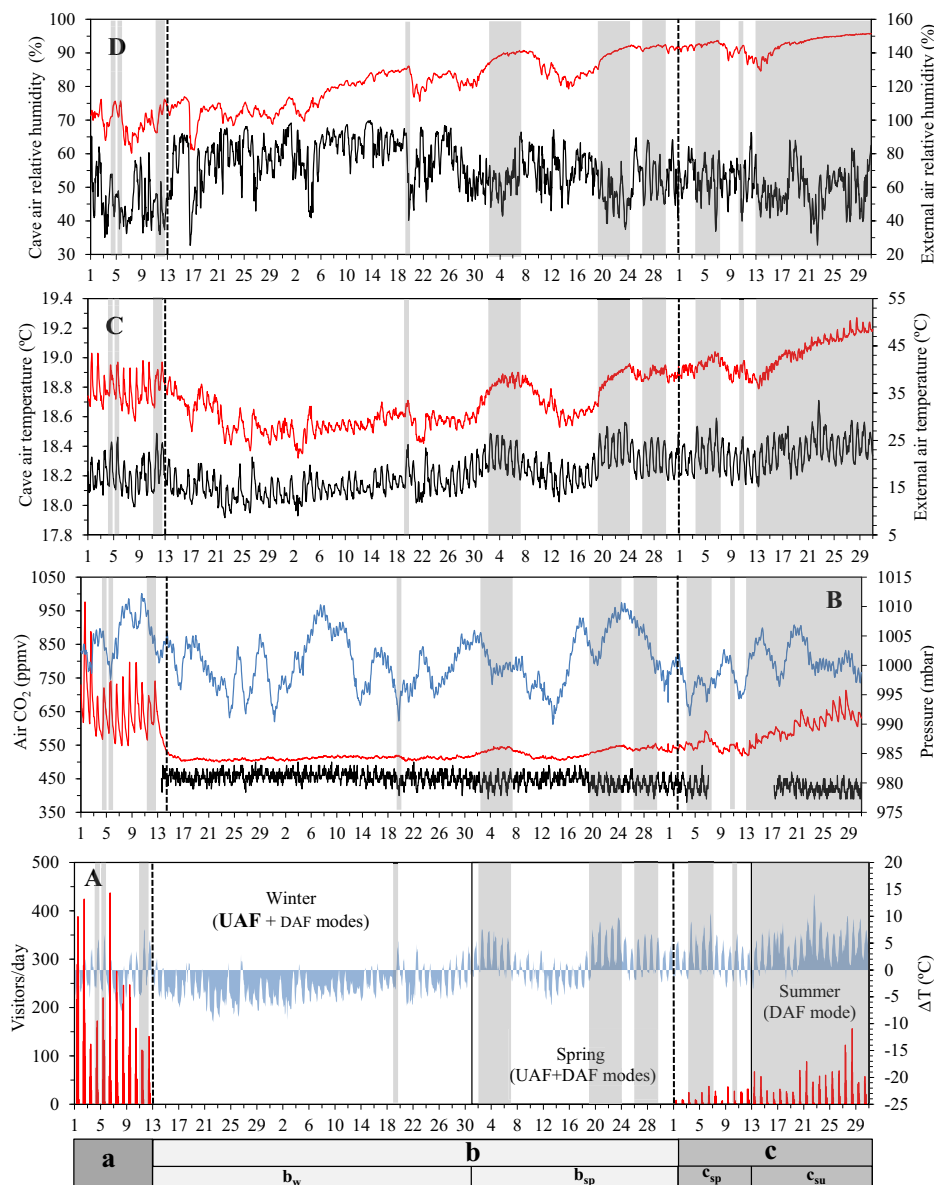


Fig. 3. Temporal evolution from 1 March to 30 June 2020 (x-axis) of different variables (hourly data). Cave data (H-3 hall) in red, external data in black. (A): daily visitors and ΔT , (B): external and cave air CO_2 concentration versus atmospheric pressure (blue), (C): cave air temperature versus external temperature and (D): cave air relative humidity versus external relative humidity. Grey bars (DAF-mode ventilation), white bars (UAF-mode ventilation). Periods differentiated: **a**- cave open, winter regime, UAF-mode ventilation predominates; **b_w**- cave closed, winter regime, UAF-mode ventilation predominates; **b_{sp}**- cave closed, spring regime, UAF and DAF-modes alternate in the cave; **c_{sp}**- cave open, spring regime, UAF and DAF-modes alternate in the cave; **c_{su}**- cave open, summer regime, DAF- mode ventilation.

cavities, which suggest the alteration of their structure and morphology (Fig. 6A, B). These precipitates are more altered than those from non-tourist sector, which have no apparent alteration features (Fig. 6C, D). Moreover, in the tourist sector, the surface is more altered in the summer precipitates (Fig. 6B). The precipitates collected in the non-tourist sector (Fig. 6C, D) and those obtained in the tourist sector during the closure period (Fig. 6E to H) show similar textures, with well-formed crystals and no cavities. No differences are observed between the texture of the precipitates formed from drip water resulting from irrigation, and later infiltrated in the cave (chamber H-3, Fig. 6E, F), together with rainwater; and those formed from meteoric drip water (chamber H-4, Fig. 6G, H). However, hydrochemical differences have been reported between these two types of water (Andreo and Carrasco, 1993; Carrasco et al., 2002).

In our study, we have observed two types of microcavities in the precipitates formed in the cave (Fig. 7): the first, (Type 1) are smaller, rounded or ellipsoidal-shaped with approximated diameter ranging from 2 to 5 μm , which is larger than the associated micro-organisms, when they are present

(Fig. 7B arrow). These microcavities have an internal structure formed by concentric lamellae and they usually appear relatively isolated on the surfaces of the crystals. Although they are much more abundant in the tourist galleries (Fig. 7B), they have also been observed in the non-tourist galleries (Fig. 7A). The second, (Type 2) are irregularly shaped, deeper and larger perforations distributed extensively on the surfaces, especially on the crystals from the tourist galleries (Fig. 7C). Their morphology raises the hypothesis that their origin could be microcavities Type 1, in a more development alteration stage, which forms cavities (Fig. 7D). As in the Type 1 microcavities, Type 2 have mostly been observed in the tourist galleries. Hence, the precipitates from visitable galleries show a greater altered appearance compared to the precipitates from the non-visitables galleries.

No significant differences between the physico-chemical parameters measured in the drip water have been observed between the pre-pandemic period (April–May 2019) and the pandemic period (April–May 2020) (Table 1). The mean values obtained for H-3 drip-water point were $\text{EC} = 1105 \mu\text{S}/\text{cm}$, $\text{pH} = 8.0$ and $Q = 5 \text{ drops}/\text{min}$ in 2019; and $\text{EC} =$

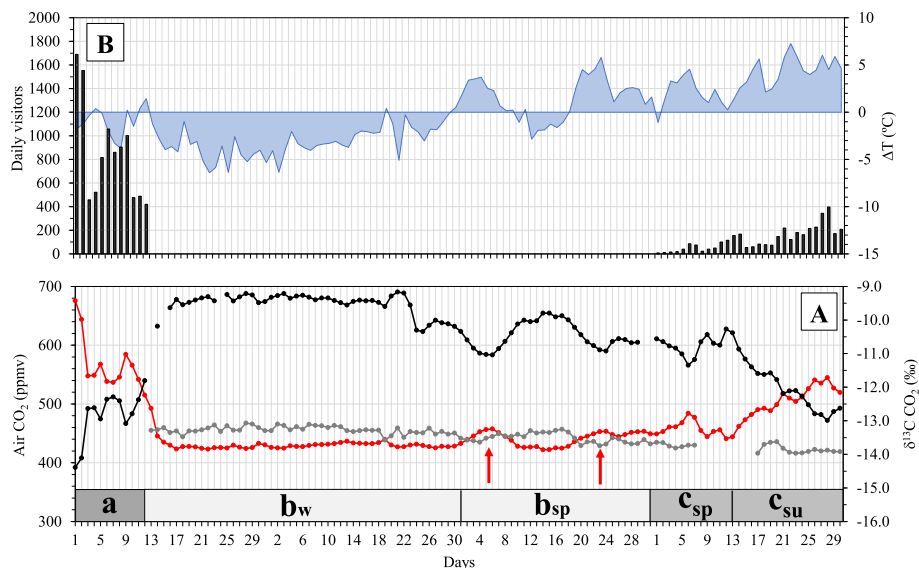


Fig. 4. Temporal evolution of (A) external air CO₂ (grey) and cave air CO₂ (red) versus isotopical signal of cave air (black). The cave data correspond to the H-3 chamber. Mean daily values from 1 March to 30 June 2020. The periods **a**, **b_w**, **b_{sp}**, **c_{sp}**, **c_{su}** and the red arrows are explained in the text and (B) daily visitors (black bars) and ΔT (blue area).

1082 μS/cm, pH = 7.8 and Q = 13 drops/min in 2020. In the case of the H-4 drip water point, the values were even more similar: 603 μS/cm, 8.2 and 4 drops/min in 2019 and 611 μS/cm, 8.2 and 4 drops/min in 2020.

5. Discussion

5.1. Microclimate parameters

The similarity between the annual evolution of the air temperature and relative humidity for 2019 and 2020 (Fig. 2A, B) indicates that neither of the parameters showed any significant changes linked to the COVID-19 pandemic. However, the cave air CO₂ concentrations showed variations linked to the decrease in the number of visitors during the pandemic period, especially during the cave closure periods (Fig. 2C). On a daily scale, changes in the temporal evolution of air temperature, cave air CO₂ concentration and, to a lesser extent, in the relative air humidity were also observed. During the periods when the cave was closed to the public, daily increases linked to the cave's lighting systems and the presence of visitors were not recorded (Fig. 3B, C).

Cave air CO₂ concentration is a balance between CO₂ influx and efflux, which is controlled by the CO₂ productivity of its source and the exchange between cave air and the external atmosphere (cave ventilation). The δ¹³C_{CO₂} data recorded in our study (H-3, tourist sector) range from -9.17 to 14.39 ‰, reflecting several CO₂ sources in the cave air with different δ¹³C signals. In the Nerja Cave, the ventilation is mainly controlled by temperature gradients between the cave air and the external air (Liñán et al., 2018, 2020). No significant differences in the natural ventilation rate of the cave for 2019 and 2020 were recorded (ΔT values were similar, Fig. 2E). However, analysis of the temporal evolution of air CO₂ shows the influence of the seasonal ventilation of the cave -ventilation regime (winter-spring-summer) and ventilation mode (UAF, DAF-) in the concentration and isotopic composition air CO₂ of the Nerja Cave.

5.1.1. Pre-pandemic period. Cave open, regular regime of visits

From 1 March to 12 March, (period **a**, pre-pandemic, with visitors), the cave chambers are under winter ventilation (Fig. 3): the airflow is strong and predominantly upward (UAF- mode). The cave air CO₂ concentrations are slightly higher (568 ppmv, -12.8 ‰, mean values) than the atmospheric level. The isotopic values are between the typical signal of the atmosphere (δ¹³C_{CO₂} ~ 7-8 ‰; e.g., Baldini et al., 2006; Vadillo et al., 2010; Matthey et al., 2016) and that corresponding to the soil (δ¹³C_{CO₂} from

-27 ‰ to -12 ‰; Deines, 1980), vadose air (-18 to -24 ‰; Matthey et al., 2016), and/or human respiration (δ¹³C_{CO₂} ~ -21 ‰; Affek and Eiler, 2006). In this period the cave air CO₂ has a double origin: atmospheric and a CO₂-rich source with lighter isotopic compositions (about -22 ‰, Fig. 5A, B) that would mostly correspond to anthropogenic CO₂. Values of 60-80 % of atmospheric air contribution in these samples show that both monitored sites (H-3, H-6) are mostly dominated by external ventilation. When the cave air CO₂ concentration increases, the isotopic signature becomes lighter (Fig. 4A), indicating a higher contribution of the anthropogenic CO₂, with lower isotopic values.

5.1.2. Pandemic period. Cave closed, no visitors

From 13 March to 30 April (period **b_w**, closure period, 0 visitors), the cave chambers continue under winter ventilation. The cave air CO₂ concentration decreases and the isotopic signal increases progressively until they reach values close to the atmosphere (429 ppmv, -9.5 ‰, mean values). It reflects the main CO₂ source, the atmosphere, and the disappearance of the anthropogenic CO₂ source (Figs. 3B, 4A). Isotopic values indicate a contribution of >90 % of atmospheric air in the studied samples, showing that both chambers (H-3, H-6) are dominated by external ventilation. As the winter period progresses, ΔT decreases. The entry of atmospheric air through the main entrances decreases, allowing us to identify (from 24 April to 30 April, Fig. 4A) the CO₂ input from the vadose zone, characterized by a lighter isotopic signal, when the ΔT is <2 °C. The fact that the cave air CO₂ concentration remains constant would indicate that the vadose zone is, at this time, a minority source of CO₂.

The isotopic signature of CO₂ source varies between the points H-3 and H-6 (Fig. 5C and D) and is lighter in the inner and deeper points (H-6). These differences might be related to the bedrock thickness above the points. Closer to the entrance, in the tourist sector, the overlying bedrock is of several tenths of meter and hence more prone to air exchange with the external atmosphere than in the inner and deeper non-tourist sectors. Seasonal air exchange with the external atmosphere and movement of vadose air is a proved process observed in boreholes located nearby (Benavente et al., 2010). This means that the CO₂ source entering the tourist galleries at this period is somehow ventilated and mixed before mixing with the cave air atmosphere.

From 1 May to 31 May (period **b_{sp}**) the cave continued closed to the public but the cave ventilation regime changes from *winter* to *spring*, as ΔT values increase and even become positive. The airflow is UAF or DAF-mode, depending on the ΔT. Cave air CO₂ values and their isotopic signal

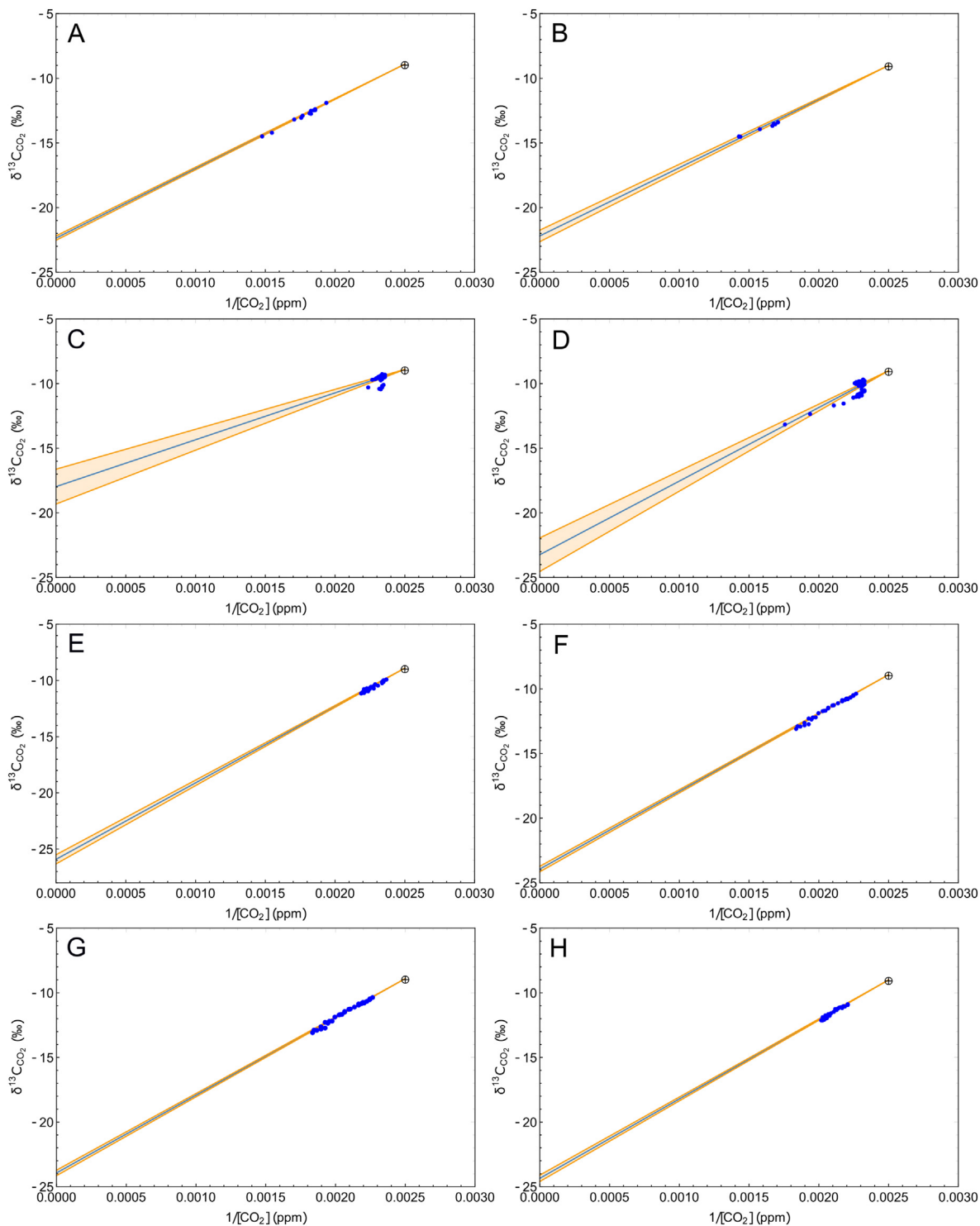


Fig. 5. Keeling plot of $\delta^{13}\text{C-CO}_2$ vs. $1/\text{CO}_2$ corresponding to data registered in: (A) H-3 chamber period a, (B) H-6 chamber, period a, (C) H-3 chamber, period b_w , (D) H-6 chamber, period b_w , (E) H-3 chamber, period b_{sp} , (F) H-6 chamber, period b_{sp} , (G) H-3 chamber, period c, (H) H-6 chamber, period c. Blue dots: cave air, crossed circles: outside air (winter).

change over the period, and two peaks with higher CO_2 values and lighter isotopic values can be observed (see arrows in Fig. 4A) coinciding with the DAF- mode ventilation periods (grey bars in Fig. 3). On the contrary, during the UAF- mode ventilation periods (e.g., from 10 to 18 May), the cave air CO_2 values are lower and the isotopic signature is heavier. During the UAF- mode, the external air enters through the lowest cave entrances and moves to the highest entrances so the main source of cave air CO_2 is the

atmosphere. However, during the DAF- mode ventilation periods, the cave air is expelled through the lowest entrances, which causes both the atmospheric air (through the higher entrances) and the air from the vadose zone to be sucked into the cave. The increase in cave air CO_2 concentration and the decrease in the isotopic signal reflect the entry of vadose air CO_2 . In this case, the atmospheric air contribution in the studied sites decreases slightly (>85 %) with respect to period b_w (>90 %), also reflecting the entry

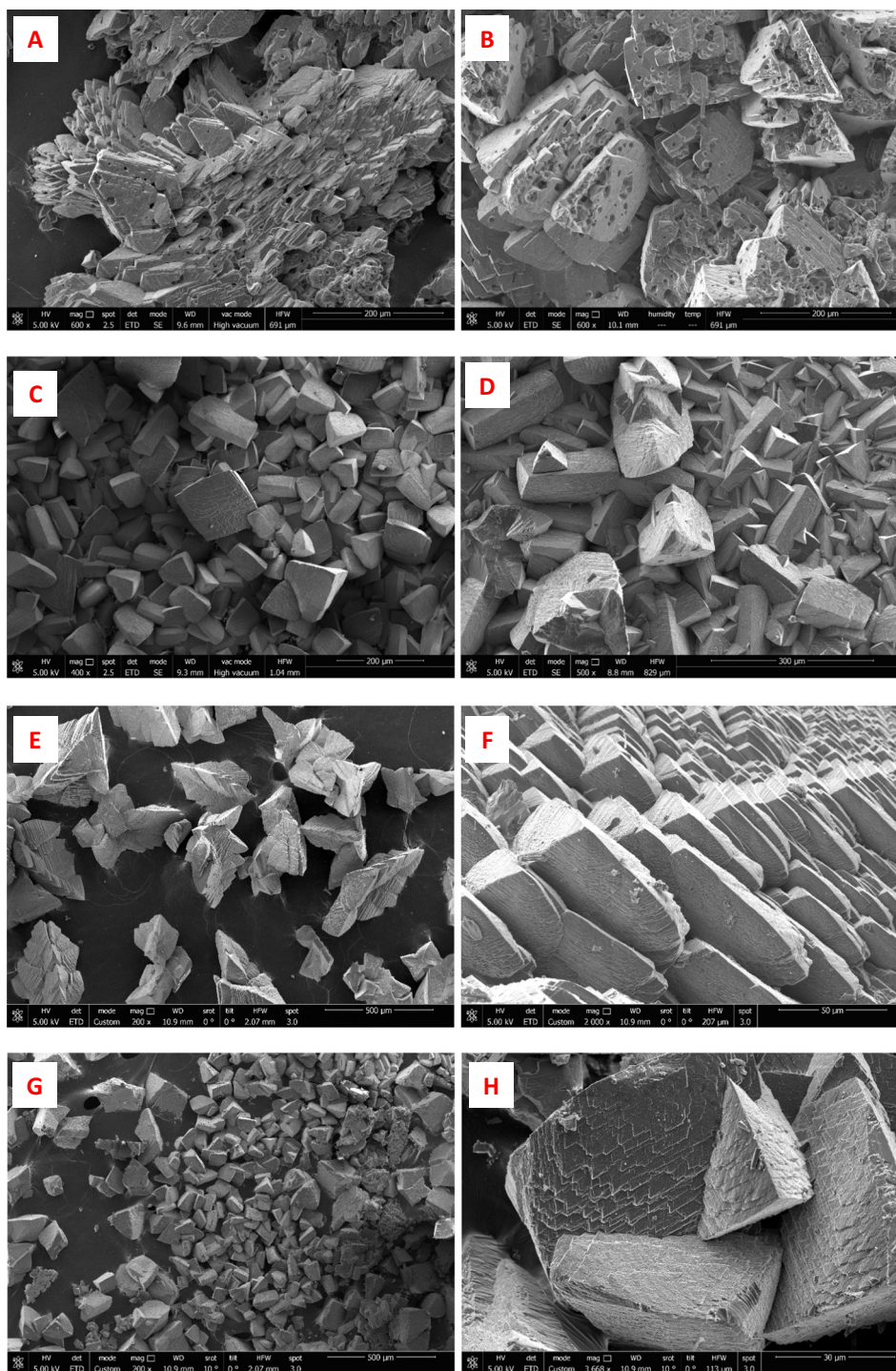


Fig. 6. (A to D) High-resolution scanning electron microscopy of carbonate precipitates formed in tourist and non-tourist chambers (A, B: H-3 hall; C: H-7 hall; D: H-5 hall) during winter (left, from December 2017 to June 2018) and summer ventilation period (right, from June to September 2018). (E to H) High-resolution scanning electron microscopy of carbonate precipitates obtained in H-3 (E, F) and H-4 (G, H) chambers during the closure period of the cave (April to May 2020, winter + spring periods). Photos scale: 200 μm (A, B, C), 300 μm (D), 500 μm (E, F), 50 μm (G) and 30 μm (H).

of vadose and soil air with a lower isotopic signal ($-26\text{‰}/-27\text{‰}$, Fig. 5E, F). In this period, characterized by a lower ventilation rate than in winter, the isotopic signature of the rich- CO_2 source in both sectors is fairly similar. Since the isotopic signature of CO_2 originating from the soil and vadose zone is similar to that of CO_2 from human respiration, it is usually challenging to discriminate between the two origins. In this case, due to the exceptional situation of the cave closure, the lighter isotopic signal is attributed only to the contribution of air from the soil and vadose zone.

5.1.3. Pandemic period. Reopening of the cave to the public

In June (period c), the cave is reopened to the public and there is a further change in the ventilation regime from *spring* (period c_{sp}) to *summer* (period c_{su}) on 13 June. During the spring period with DAF-ventilation mode, we observed increases in cave air CO_2 concentration and simultaneous decreases in the isotopic signal, indicating the entry of vadose air CO_2 . Once the summer cave ventilation regime is established (period c_{su}), the cave air CO_2 concentration increases progressively up to values above 500 ppmv. The isotopic signal becomes lighter up to a minimum value of

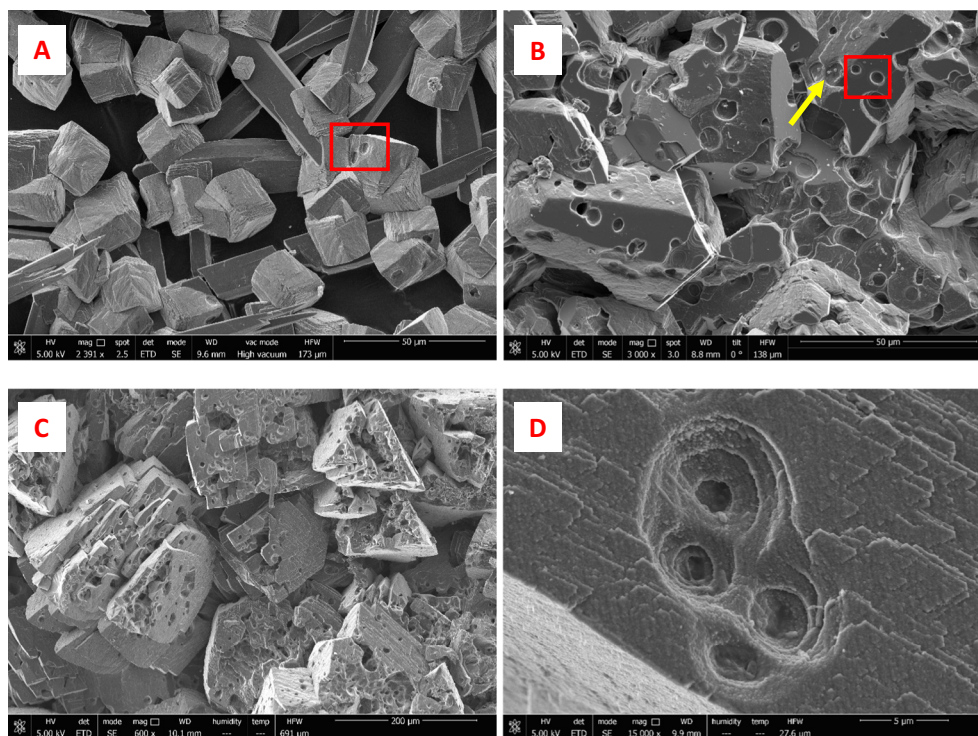


Fig. 7. Microcavities observed in the Nerja Cave precipitates. Type 1 (red squares): smaller, spherical-shaped ones with concentric laminae in (A): non-visitable sector (H-6, cave open) and (B): tourist sector (H-4 hall, cave open). The arrow indicates the presence of micro-organisms. Type 2: irregularly shaped, deeper and larger perforations distributed extensively on the surfaces in (C): tourist sector (H-3, cave open). Fig. D shows the detail of the Type 2 cavity as a result of adding several Type 1 microcavities. Note the different scales of the photos (A, B: 50 µm; C: 200 µm; D: 5 µm).

– 13.0 ‰. In this case, the lighter isotopic signal cannot only be attributed to air from the soil and vadose zone but also to exhaled air from the visitors. Values of 75–90 % of atmospheric air contribution also show a decrease in the external ventilation and a CO₂-rich gas with a heavier isotopic composition than period *b_{sp}* (about –24 ‰, Fig. 5G, H), reflecting the addition of the anthropogenic source of CO₂ (with more enriched values) to the vadose input.

5.2. Carbonate precipitation

Regarding the carbonate precipitates, and regardless of the ventilation regime of the cave, we observed: a) during periods when the cave is open to the public, the precipitates from the Tourist Galleries are formed by crystals that show many traces of dissolution and a higher presence of micro-organisms. The precipitates formed in the non-tourist sector show hardly

Table 1

Summary of electrical conductivity (EC, in µS/cm), pH and drip-water flow (Qd, as number of drops/min) values measured in the drip water at precipitation sites H-3 and H-4 (water stored in the Petri dishes) from April to May of 2019 and 2020. In italics, mean values for each parameter.

Date	H-3			H-4			
	EC	pH	Qd	EC	pH	Qd	
Pre-pandemic period	15-4-19	1110	4	620		4	
	30-4-19	1070	8.1	590	8.4	4	
	17-5-19	1070	7.9	5	600	8.2	4
	28-5-19	1170	8.0	5	600	8.3	4
	<i>Mean</i>	<i>1105</i>	<i>8.0</i>	<i>5</i>	<i>603</i>	<i>8.3</i>	<i>4</i>
Pandemic period	13-4-20	1150	7.8	15	580	8.3	4
	21-4-20	1110	7.7	14	590	8.2	3
	04-5-20	1110	7.7	13	666	8.0	3
	22-5-20	1040	7.9	12	570	8.2	4
	27-5-20	1050	7.9		640	8.2	
	28-5-20	1030	7.9	10	620	8.2	4
	<i>Mean</i>	<i>1082</i>	<i>7.8</i>	<i>13</i>	<i>611</i>	<i>8.2</i>	<i>4</i>

any traces of alteration and the presence of micro-organisms is occasional; b) during the periods when the cave is closed to the public, the precipitates in the tourist galleries are formed by crystals without abundant traces of dissolution and there is no presence of micro-organisms.

Cave micro-organisms can induce dissolution processes, through the excretion of acids, or carbonate precipitation, via biomineralization processes (Cañaveras et al., 2001; Cuezva et al., 2009, 2012; Cacchio et al., 2003, 2004; Pacton et al., 2013). In the Nerja Cave, Jiménez de Cisneros et al. (2020) related the dissolution morphologies and the abundance of micro-organisms in the precipitates formed in the tourist sector to the distinctive vegetation cover over this cave sector (anthropized soils) and micro-organisms from anthropogenic activity. Later, Jurado et al. (2022) studied the microbial communities in carbonate precipitates of the Nerja Cave and identified 19 out of 46 bacterial genera related to the carbonate precipitation/dissolution cycle and, therefore, with a potential role in mineral deposition/dissolution. However, the low number of micro-organisms compared to the microcavities observed in the precipitates leads us to reject the hypothesis of microcavity development by bacterial dissolution. Bissett et al. (2011) investigated the ability of bacterial communities to colonise and dissolve carbonate substrates. They found no evidence of bacterial-mediated carbonate dissolution despite the bacterial communities rapidly and densely colonising the tested substrates. Therefore, they concluded that the probability that the metabolism of the colonising bacteria led to significant carbonate dissolution was very low.

Suchy et al. (2020) identified perforations with similar appearance to Type 1 micro-perforations observed in the Nerja Cave in opal deposits preserved in speleothems of the Koněprusy Caves (Czech Republic), attributing them to the presence of microbes that acted as nucleation sites and/or templates for opal precipitation. Pedley and Rogerson (2010), in a mesocosm experiment, also identified perforations on calcite crystals which were occupied during their development by EPS (extracellular polymeric substances) strands and frequently by small coccoid bacteria. The morphologies observed in the experiment of Pedley and Rogerson (2010), are similar to Type 1 micro-perforations observed in the Nerja

Cave but, in our case, we did not observe micro-perforations occupied by micro-organisms, EPSs or anything similar.

Based on the above investigations, we think that the Type 1 micro-perforations could be related to the sedimentation of airborne fungi spores and heterotrophic bacteria on the dishes (Novakova et al., 2014; Jurado et al., 2021) at the same time as abiotic calcite precipitation occurs, since their size is compatible with that of the microcavities (2–5 μm diameter). Thus, first the perforations in the calcite crystals were occupied by spores/bacteria that would act as the EPS described by Pedley and Rogerson (2010).

Previous research identified airborne spores of *Penicillium*/*Aspergillus* and *Bacillus*/*Micrococcus* as the most abundant airborne genus (spores and bacterial, respectively) in the Nerja Cave (Del Rosal et al., 2007, 2014; Docampo et al., 2010, 2011; Jurado et al., 2021). Moreover, in the tourist galleries generally there is a much higher presence of airborne spores than in the non-tourist galleries linked to the cave ventilation but also to human activity and the presence of visitors, which affect the air mobilisation and dispersal of aerial micro-organisms (Shapiro and Pringle, 2010; Docampo et al., 2010, 2011). According to Pedley and Rogerson (2010), this could explain the higher abundance of this type of microcavity in the tourist sector compared to the non-tourist area during the opening periods of the cave and their low incidence in the precipitates of the tourist sector during the closure period of the cave. Moreover, the short exposition time of Petri dishes during the closure period (1 month) would imply a lower decantation of micro-organisms or spores on the dishes and, consequently, a lower presence of microcavities.

The lack of nutrients in the Petri dishes and the accumulation of drip water inside them would prevent the development of these micro-organisms and, finally, their viability. Both factors could explain why Jurado et al. (2022) only identified *Bacillus* (and with low relative abundance) and did not identify any fungi micro-organism in the preliminary metagenomic research of the carbonate precipitates from the Nerja Cave. These results suggest the scarce or null contribution of airborne bacteria or fungi in the carbonate precipitates of this cave, according to the results obtained by Ikner et al. (2007) and Leuko et al. (2017), who investigated the microbial diversity on rock and speleothem surfaces in the Kartchner show Caverns (USA) and Su Bentu Cave (Italy).

The shape and range of the larger microcavities (Type 2) do not seem to correspond to the footprints of micro-organism presence but rather to abiotic dissolution processes after crystal formation. In general, the number of micro-organisms observed in the carbonate precipitates seems too low to produce the widespread dissolution observed in them. In SEM images, where this type of microcavity is abundant micro-organisms are very rare or absent (Figs. 6B, 7C), which leads us to rule out biotic dissolution as the main process generating the Type 2 microforms.

Infiltrating water moving from the surface to caves continuously interacts with the gaseous and solid phases of the soil and vadose zone. The pCO_2 in the vadose zone of Nerja Cave is relatively high (35,500 $\mu\text{L/L}$), as shown by hydrogeochemical modelling (Benavente et al., 2010) supported by experimental measurements in the boreholes of the research site near the cave (Fig. 1). Thus, the percolating water increases its CO_2 levels and dissolves carbonate minerals in the rock. When the CO_2 -saturated vadose water reaches the cave, it can degas if its pCO_2 is higher than the pCO_2 of the cave air. A high pCO_2 gradient between the cave air and the drip water would enhance the CO_2 degassing and the concomitant carbonate deposition, favouring the precipitation of CaCO_3 from the solution due to higher supersaturation. On the contrary, relatively high pCO_2 levels inside the cave would reduce the driving force for carbonate precipitation, eventually causing corrosion of the existing speleothem formations.

The CO_2 exhaled by the visitors increases the cave air pCO_2 and water pCO_2 , as the gas is dissolved in it. During the periods of time when the cave is open to the public, the precipitates in the tourist galleries show dissolution features. The precipitates formed in the non-tourist galleries, and those formed in the tourist galleries when the cave is closed to the public do not show traces of dissolution. Accordingly, it could be thought that

there is a relationship between the dissolution morphologies observed in the crystals and the presence of visitors in the cave.

Higher pCO_2 levels increases acidity of the condensed water along the cave walls and higher temperatures enhance faster reaction rates (Vieten et al., 2016), increasing the carbonate dissolution rate during the tourist period. In the Postojna Cave (Slovenia), Kukuljan et al. (2021) attributed the dissolutional features to the high and highly-variable concentrations of CO_2 in the air of one of its non-tourist chambers. Liñán et al. (2021) reported the existence of “corrosion condensation” processes in the Tourist Galleries of the Nerja Cave during periods with very high relative humidity values (98 %) and high pCO_2 levels. Thus, this process of corrosion by condensation could act and produce microcavities in the initial moments of mineral precipitation, e.g., when the Petri dishes under the drip point (with crystals already formed) are not entirely covered with water. However, we have ruled out a significant contribution of this process in the genesis of Type 2 micro-perforations. During the winter ventilation regime, the precipitates formed in the non-tourist chambers are subjected to CO_2 and relative air humidity values equivalent to (or higher, in the case of the latter parameter) than those of the tourist sector (Fig. 2C). Nevertheless, dissolution morphologies are practically non-existent in the crystals of the non-tourist chambers, even though the drip flow rates in several points are lower and, therefore, the exposure time to the cave atmosphere of the crystals already formed is longer compared to those of the tourist sector (the dish takes more time to be completely covered with water).

Although during the winter, spring and autumn ventilation regimes the mean daily cave air CO_2 concentrations are similar in both the tourist and the non-tourist sectors (Fig. 2C), there is a significant difference between the hourly values (Fig. 8). This difference is more remarkable during the summer period (Fig. 8A) when the DAF-ventilation mode is set in the cave and the air from the tourist sector does not reach the non-tourist area. According to this, in the tourist galleries, and throughout the year, the daily increase in air CO_2 in contact with the drip water collected in the Petri dishes would induce an increase in dissolved gaseous CO_2 . In turn, this process would increase the acidity of the drip water and thus the ability to dissolve the carbonate precipitates with which it is in contact. The CO_2 decrease in the air would produce the opposite effect: the degassing of the water and the carbonate precipitation.

In the non-tourist sector, we recorded relatively significant daily increases in the CO_2 concentration in the air of H-5 hall, the nearest to the tourist sector, during the UAF-mode ventilation (Fig. 8B). These increases (about 300 ppmv of mean value from 1 to May 15, 2016), lower than those recorded in the tourist sector (about 140 ppmv of mean value for the same period), would not be sufficient to dissolve the carbonate crystals previously formed on the Petri dishes. Therefore, we would not be able to observe dissolution features. During the closure period to the public, the air CO_2 concentrations in the tourist sector do not show daily increases (Fig. 8B). They are similar to those recorded in the non-tourist sector during the summer period (Fig. 8A). The different daily evolution of air CO_2 concentration recorded in different cave sectors and in different time periods would explain why dissolution morphologies on crystals are not observed in either the non-tourist galleries or the tourist sector when the cave is closed to the public. Thus, the air CO_2 concentration appears to be a critical factor in the formation of the extensive dissolution morphologies observed on the crystals formed on the dishes.

6. Conclusions

The cave closure period to the public caused by the pandemic (COVID-19) has provided a unique opportunity to study the variations in microclimate conditions and carbonate precipitation in an important karst tourist cave (Nerja, SE Spain) without the presence of visitors. After the closure of the cave to the public, the cave air CO_2 concentration decreased to near the atmospheric values reflecting the main source of CO_2 in the cave air (atmosphere, contribution >85–90 %) and the disappearance of the anthropogenic source of CO_2 , although it was also possible to identify and, for the first time, isotopically characterise the input of soil and vadose air

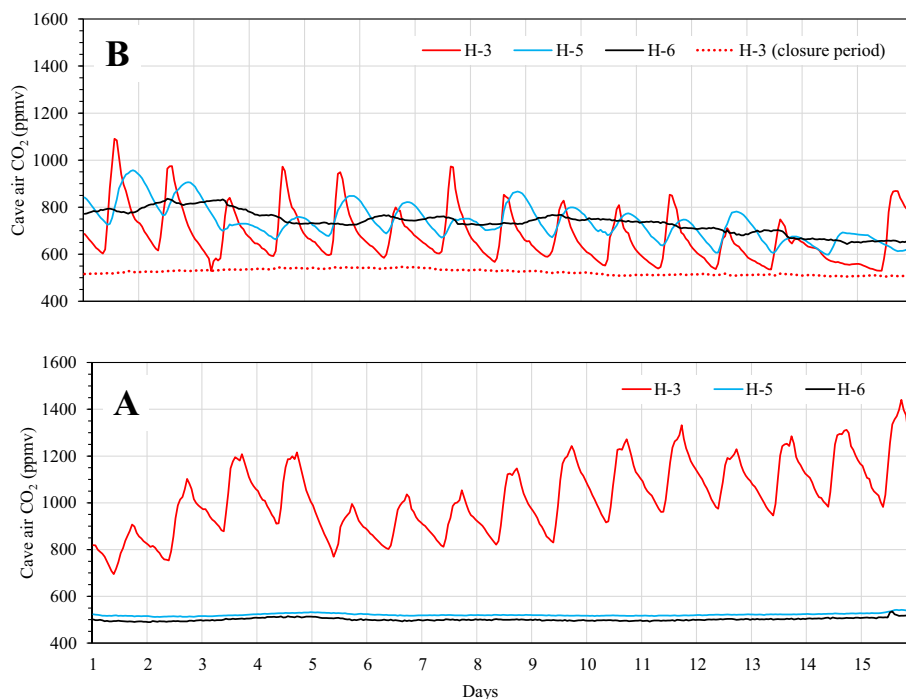


Fig. 8. Hourly air CO₂ concentration in the Nerja Cave in the Tourist Galleries and non-tourist area from 1 to 15 May 2016 (Fig. 8B, UAF mode); and from 1 to 15 August 2016 (Fig. 8A, DAF mode). We represent data from 2016 (rather than 2019 or 2020 data) because the microclimate station in chamber H-5 was closer to the drip-water point than in later years (when the station's location was changed). Fig. 8B includes the data recorded in the Tourist Galleries from 1 to 15 May 2020, during the closure period (discontinuous red line).

($\delta^{13}\text{C}_{\text{CO}_2} = -26\text{‰}/-27\text{‰}$) during the ventilation periods in DAF-mode. Thanks to the particular conditions imposed by the pandemic it has been possible to verify the significant effect of human respiration on the isotopic signature of the cave air. During the cave closure period, the mean cave air CO₂ concentration (434 ppmv) was 1.8 times lower than during the same period in 2019 (781 ppmv), when the cave was open to the public.

The texture of the precipitates formed in the tourist sector during the cave closure period was similar to that of the precipitates formed in the non-tourist sector, without any significant changes being detected in the physico-chemical characteristics of the drip water. The precipitates have well-formed crystals and no cavities, in contrast to the precipitates formed in the tourist galleries during the opening periods of the cave, which show abundant dissolution morphologies (microcavities).

The genesis of these microcavities could be linked to natural and anthropic factors. The Type 1 microcavities may have a biotic origin, related to the sedimentation of airborne fungi spores and bacteria on the Petri dishes simultaneously with the abiotic calcite precipitation. The anthropogenic CO₂ would enlarge microcavities of biotic origin, causing the Type 2 microcavities. Thus, this shows a clear influence of anthropogenic CO₂ on the genesis of the extensive dissolution features affecting the carbonate crystals and, therefore, it alerts us about the possible corrosion phenomena that would affect the speleothems located in the visitable galleries of tourist caves, especially in those with low ventilation rates or/and a high number of visitors.

CRediT authorship contribution statement

C. Liñán: Conceptualization, Methodology, Formal analysis, Investigation, Writing – original draft, Writing – review & editing, Visualization, Supervision. **C. Jiménez de Cisneros:** Conceptualization, Methodology, Formal analysis, Investigation, Resources, Writing – review & editing, Visualization, Supervision. **J. Benavente:** Conceptualization, Investigation, Writing – review & editing, Supervision. **I. Vadillo:** Conceptualization, Methodology, Investigation, Resources, Writing – review & editing, Supervision. **Y. del Rosal:** Investigation, Formal analysis, Writing – original

draft, Writing – review & editing. **L. Ojeda:** Methodology, Formal analysis, Investigation, Data curation, Writing – original draft, Writing – review & editing, Visualization.

Data availability

Data will be made available on request.

Declaration of competing interest

The authors declare that they have no known competing financial interests or personal relationships that could have appeared to influence the work reported in this paper.

Acknowledgments

Funding charge open access: University of Malaga / CBUA. This work is the result of the studies performed by the Geology area of the General Project for Interdisciplinary Research of the Nerja Cave, which is specifically aimed at the conservation of the cavity. It is financed by the Nerja Cave Foundation, co-ordinated by its Research Institute and authorized by the Consejería de Cultura (Junta de Andalucía). This study is also a contribution to the Research Groups RNM-308 and RNM-126 of the Junta de Andalucía and to the Projects PID2021-125619OB-C21, PID2021-125619OB-C22, TED2021-130549B-I00 funded by MCIN/AEI/10.13039/501100011033. The authors thank Angela Tate for revising the English text and two anonymous reviewers who have contributed to improving this article.

References

- Affek, H.P., Eiler, J.M., 2006. Abundance of mass 47 CO₂ in urban air, car exhaust, and human breath. *Geochim. Cosmochim. Acta* 70, 1–12.
- Andreo, B., Carrasco, F., 1993. Estudio geoquímico de las aguas de infiltración de la Cueva de Nerja. In: Carrasco, F. (Ed.), *Geología de la Cueva de Nerja*. 3. Patronato de la Cueva de Nerja, pp. 299–328.

- Andreo, B., Barberá, J.A., Mudarra, M., Marín, A.I., García-Orellana, J., Rodellas, V., Pérez, I., 2018. A multi-method approach for groundwater resource assessment in coastal carbonate (karst) aquifers: the case study of Sierra Almijara (southern Spain). *Hydrogeol. J.* 26 (1), 41–56.
- Baldini, J.U.L., Baldini, L.M., McDermott, F., Clipson, N., 2006. Carbon dioxide sources, sinks and spatial variability in shallow temperate zone caves: evidence from Ballynamindra Cave, Ireland. *J. Cave Karst Stud.* 68 (1), 4–11.
- Benavente, J., Vadillo, I., Carrasco, F., Soler, A., Liñán, C., Moral, F., 2010. Air carbon dioxide contents in the vadose zone of a Mediterranean karst. *Vadose Zone J.* 9, 126–136. <https://doi.org/10.2136/vzj2009.0027>.
- Bissett, A., Neu, T.R., de Beer, D., 2011. Dissolution of calcite in the twilight zone: bacterial control of dissolution of sinking planktonic carbonates is unlikely. *PLoS ONE* 6 (11), e2604. <https://doi.org/10.1371/journal.pone.0026044>.
- Cacchio, P., Ercole, C., Cappuccio, G., Lepidi, A., 2003. Calcium carbonate precipitation by bacterial strains isolated from a limestone cave and from a loamy soil. *Geomicrobiol. J.* <https://doi.org/10.1080/01490450303883>.
- Cacchio, P., Contento, R., Ercole, C., Cappuccio, G., Preite Martinez, M., Lepidi, A., 2004. Involvement of microorganisms in the formation of carbonate speleothems in the Cervo cave (L'Aquila - Italy). *Geomicrobiol. J.* <https://doi.org/10.1080/01490450490888109>.
- Cañaveras, J.C., Sánchez-Moral, S., Soler, V., 2001. Microorganisms and microbially induced fabrics in cave walls. *Geomicrobiol. J.* 18, 223–240.
- Carrasco, F., Vadillo, I., Liñán, C., Andreo, B., Durán, J.J., 2002. Control of environmental parameters for management and conservation of Nerja Cave (Malaga, Spain). *Acta Carsologica* 31 (1), 105–122. <https://doi.org/10.3986/ac.v31i1.407>.
- Cuevas, S., Sanchez-Moral, S., Saiz-Jimenez, C., Cañaveras, J., 2009. Microbial communities and associated mineral fabrics in Altamira cave, Spain. *Int. J. Speleol.* <https://doi.org/10.5038/1827-806X.38.1.9>.
- Cuevas, S., Fernández-Cortés, A., Porca, E., Lejla, P., Jurado, V., Serrano-Ortiz, P., Hermosin, B., Cañaveras, J.C., Saiz-Jimenez, C., Hernandez-Marine, M., Sanchez-Moral, S., 2012. The biogeochemical role of Actinobacteria in Altamira Cave, Spain. *FEMS Microbiol. Ecol.* <https://doi.org/10.1111/j.1574-6941.2012.01391.x>.
- Deines, P., 1980. The isotopic composition of reduced organic carbon. In: Fritz, P., Fontes, J. (Eds.), *Handbook of Environmental Isotope Geochemistry*. Springer Nature, pp. 329–406.
- Del Rosal, Y., Martínez-Manzanares, E., Marín, F., Liñán, C., Simón, M.D., 2007. Análisis de la calidad microbiológica aérea en el interior de la Cueva de Nerja. In: Durán, J.J., Robledo, P.A., Vázquez, J. (Eds.), *Cuevas turísticas: aportación al desarrollo sostenible*. IGME, Madrid, pp. 181–190.
- Del Rosal, Y., Liñán, C., Hernández-Marín, M., 2014. The conservation of the Nerja Cave: preserving anthropogenic impact in a tourist cave. In: Saiz-Jimenez, C. (Ed.), *The Conservation of Subterranean Cultural Heritage*. CRC Press/Balkema, Leiden, pp. 193–206.
- Docampo, S., Trigo, M.M., Recio, M., Melgar, M., García-Sánchez, J., Calderon-Ezquerro, M.C., Cabezu, B., 2010. High incidence of Aspergillus and Penicillium spores in the atmosphere of the cave of Nerja (Malaga, southern Spain). *Aerobiologia* 26, 89–98.
- Docampo, S., Trigo, M.M., Recio, M., Melgar, M., García-Sánchez, J., Cabezu, B., 2011. Fungal spores content of the atmosphere of the cave of Nerja (southern Spain): diversity and origin. *Sci. Total Environ.* 409, 835–843.
- Dragovich, D., Grose, J., 1990. Impact of tourist on carbon dioxide levels at jenolan caves, Australia: an examination of microclimatic constraints on tourist cave management. *Geoforum* 21 (1), 111–120.
- Dreybrodt, W., 2000. Equilibrium chemistry of karst waters in limestone terranes. In: Klimchouk, A.B., Ford, D.C., Palmer, A.N., Dreybrodt, W. (Eds.), *Speleogenesis, Evolution of Karst Aquifers*. National Speleological Society, Huntsville (Alabama, USA), pp. 126–135.
- Dreybrodt, W., Eisenlohr, L., 2000. Limestones dissolution: rates in karst environments. In: Klimchouk, A.B., Ford, D.C., Palmer, A.N., Dreybrodt, W. (Eds.), *Speleogenesis, Evolution of Karst Aquifers*. National Speleological Society, Huntsville (Alabama, USA), pp. 136–148.
- Fernández, P.L., Gutierrez, I., Quindós, L.S., Soto, J., Villar, E., 1986. Natural ventilation of the paintings room in the Altamira cave. *Nature* 321 (5), 586–588.
- Hoyos, M., Soler, V., Sánchez-Moral, S., Cañaveras, J.C., Sanz-Rubio, E., 1998. Carbon dioxide fluxes in karstic caves (Altamira and Tito Bustillo caves, Spain). In: Daoxian, Y., Cheng, Z. (Eds.), *Karst Processes and the Carbon Cycle: Final Report of IGCP 379 (2002)*, pp. 80–81.
- Houillon, N., Lastennet, R., Denis, A., Malaurent, P., Minvielle, S., Peyraube, N., 2017. Assessing cave internal aereology in understanding carbon dioxide (CO₂) dynamics: implications on calcite mass variation on the wall of Lascaux Cave (France). *Environmental Earth Sciences* 76 (4), 170. <https://doi.org/10.1007/s12665-017-6498-8> February 2017.
- Ikner, L.A., Toomey, R.S., Nolan, G., Neilson, J.W., Pryor, B.M., Maier, R.M., 2007. Culturable microbial diversity and the impact of tourism in Kartchner Caverns, Arizona. *Microb. Ecol.* 53, 30–42. <https://doi.org/10.1007/s00248-006-9135-8>.
- Jiménez de Cisneros, C., Peña, A., Caballero, E., Liñán, C., 2020. A multiparametric approach for evaluating the current carbonate precipitation and external soil of Nerja Cave (Málaga, Spain). *Int. J. Environ. Res.* 15, 1–13. <https://doi.org/10.1007/s41742-020-00278-x>.
- Jurado, V., Del Rosal, Y., Liñán, C., Martín-Pozas, T., Gonzalez-Pimentel, J.L., Saiz-Jimenez, C., 2021. Diversity and seasonal dynamics of airborne fungi in Nerja Cave, Spain. *Appl. Sci.* 11 (13), 6236. <https://doi.org/10.3390/app11136236>.
- Jurado, V., Del Rosal, Y., Jimenez de Cisneros, C., Liñán, C., Martín-Pozas, T., Gonzalez-Pimentel, J.L., Hermosin, B., Saiz-Jimenez, C., 2022. Microbial communities in carbonate precipitates from drip waters in Nerja Cave, Spain. *PeerJ* 10, e13399. <https://doi.org/10.7717/peerj.13399>.
- Keeling, C.D., 1958. The concentration and isotopic abundances of atmospheric carbon dioxide in rural areas. *Geochim. Cosmochim. Acta* 13 (4), 322–334.
- Koning, K., McFarlane, R., Gosse, J.T., Lawrence, S., Carr, L., Horne, D., Van Wagoner, N., Boddy, C.N., Cheeptham, N., 2022. Biomining in cave bacteria-popcorn and soda straw crystal formations, morphologies, and potential metabolic pathways. *Front. Microbiol.* 13. <https://doi.org/10.3389/fmicb.2022.933388>.
- Kukuljan, L., Gabrovšek, F., Johnston, V., 2021. Low calcium cave dripwaters in a high CO₂ environment: formation and development of corrosion cups in Postojna Cave, Slovenia. *Water* 13, 3184. <https://doi.org/10.3390/w13223184>.
- Leuko, S., Koskinen, K., Sanna, L., D'Angeli, I.M., De Waele, J., Marcia, P., Moissl-Eichinger, C., Rettberg, P., 2017. The influence of human exploration on the microbial community structure and ammonia oxidizing potential of the Su Bentu limestone cave in Sardinia, Italy. *PLoS ONE* 12 (7), e0180700. <https://doi.org/10.1371/journal.pone.0180700>.
- Liñán, C., Simón, M.D., del Rosal, Y., Garrido, A., 2007. Estudio preliminar del clima en el entorno de la Cueva de Nerja (Andalucía, provincia de Málaga). In: Durán, J.J., Robledo, P., Vázquez, J. (Eds.), *Cuevas turísticas: aportación al desarrollo sostenible*. 24. Publicaciones del IGME, serie Hidrogeología y aguas subterráneas, pp. 159–168.
- Liñán, C., del Rosal, Y., Cantos, F., Vadillo, I., Benavente, J., Ojeda, L., 2018. Highlighting the importance of transitional ventilation regimes in the management of Mediterranean show caves (Nerja-Pintada system, southern Spain). *Sci. Total Environ.* 631–632, 1268–1278. <https://doi.org/10.1016/j.scitotenv.2018.02.304>.
- Liñán, C., Ojeda, L., Benavente, J., del Rosal, Y., Vadillo, I., Carrasco, F., 2020. Coupling air temperature records and gravimetric data to interpret ventilation patterns in a Mediterranean karstic system (Nerja-Pintada caves, southern Spain). *Science of the Total Environment* 730, 139147. <https://doi.org/10.1016/j.scitotenv.2020.139147> ISSN 0048-9697.
- Liñán, C., Benavente, J., del Rosal, Y., Vadillo, I., Ojeda, L., Carrasco, F., 2021. Condensation water in heritage touristic caves: isotopic and hydrochemical data and a new approach for its quantification through image analysis. *Hydrol. Process.* 35, e14083. <https://doi.org/10.1002/hyp.14083>.
- Mattey, D.P., Atkinson, T.C., Barker, J.A., Fisher, R., Latin, J.P., Durrell, R., Ainsworth, M., 2016. Carbon dioxide, ground air and carbon cycling in Gibraltar karst. *Geochim. Cosmochim. Acta* 184, 88–113.
- Mulec, J., 2014. Human impact on underground cultural and natural heritage sites, biological parameters of monitoring and remediation actions for insensitive surfaces: case of Slovenian show caves. *J. Nat. Conserv.* 22 (2), 132–141. <https://doi.org/10.1016/j.jnc.2013.10.001>.
- Mulec, J., Oarga-Mulec, A., Šturm, S., Tomazin, R., Matos, T., 2017. Spatio-temporal distribution and tourist impact on airborne bacteria in a cave (Škocjan Caves, Slovenia). *Diversity* 9 (3), 28. <https://doi.org/10.3390/d9030028>.
- Novakova, A., Hubka, V., Saiz-Jimenez, C., 2014. Microscopic fungi isolated from cave air and sediments in the Nerja Cave - preliminary results. In: Saiz-Jimenez, C. (Ed.), *The Conservation of the Subterranean Cultural Heritage*. CRC Press Balkema, pp. 239–245. <https://doi.org/10.1201/b17570-29>.
- Ojeda, L., Vadillo, I., Liñán, C., Fóster, S., Carrasco, F., Villodres, F.M., Jimena, D., Atencia, A., Benavente, J., 2018. Acondicionamiento e instalación de un equipo de espectroscopia láser (CO₂, CH₄, δ13CCO₂ y δ13CCH₄) en la cueva de Nerja (Málaga, España). In: Robledo, P., Durán, J.J. (Eds.), *Cuevas: la flecha del tiempo, de la prehistoria a la actualidad*. ACTE, pp. 253–264.
- Ojeda, L., Vadillo, I., Etiope, G., Benavente, J., Liñán, C., del Rosal, Y., Tapia, S.T., Morfínigo, M.A., Carrasco, F., 2019. Methane sources and sinks in karst systems: The Nerja cave and its vadose environment (Spain). *Geochim. Cosmochim. Acta* 259, 302–315. <https://doi.org/10.1016/j.gca.2019.06.011> ISSN 0016-7037.
- Pacton, M., Breitenbach, S., Lechleitner, F., Vaks, A., Rollion-Bard, C., Gutareva, O., Osintsev, A., Vasconcelos, C., 2013. The role of microorganisms in the formation of a stalactite in botovskaya cave, Siberia - paleoenvironmental implications. *Biogeosciences* 10, 6115–6130. <https://doi.org/10.5194/bg-10-6115-2013>.
- Pataki, D.E., Ehleringer, J.R., Flanagan, L.B., Yakir, D., Bowling, D.R., Still, C.J., Buchmann, N., Kaplan, J.O., Berry, J.A., 2003. The application and interpretation of Keeling plots in terrestrial carbon cycle research. *Glob. Biogeochem. Cycles* 17 (1), 22–15.
- Pedley, H.M., Rogerson, M., 2010. In Vitro Investigations of the Impact of Different Temperature and Flow Velocity Conditions on Tufa Microfabric Tufas and Speleothems: Unravelling the Microbial and Physical Controls. Geological Society of London. Special Publications, London <https://doi.org/10.1144/SP336.9>.
- Sánchez-Moral, S., Soler, V., Cañaveras, J.C., Sanz-Rubio, E., Van Grieken, R., Gysels, K., 1999. Inorganic deterioration affecting the Altamira Cave, N Spain: quantitative approach to wall-corrosion (solution etching) processes induced by visitors. *Sci. Total Environ.* 243–244, 67–84. [https://doi.org/10.1016/S0048-9697\(99\)00348-4](https://doi.org/10.1016/S0048-9697(99)00348-4).
- Sanchidrián, J., Valladas, H., Alcaide, M.A., Pons-Branchu, E., Quiles, A., 2017. New perspectives for 14C dating of parietal markings using CaCO₃ thin layers: an example in Nerja Cave (Spain). *J. Archaeol. Sci. Rep.* 12, 74–80. <https://doi.org/10.1016/j.jasrep.2017.01.028>.
- Shapiro, J., Pringle, A., 2010. Anthropogenic influences on the diversity of fungi isolated from caves in Kentucky and Tennessee. *Am. Midl. Nat.* 76–86. <https://doi.org/10.1674/0003-0031-163.1.76>.
- Suchy, V., Borecka, L., Pachnerova, B., Havelcová, M., Svetlík, I., Machovič, V., Lapčák, L., Ovšonková, Z., 2020. Microbial signatures from speleothems: a petrographic and scanning electron microscopy study of coralloids from the Koněprusy Caves (the Bohemian Karst, Czech Republic). *Sedimentology* 68. <https://doi.org/10.1111/sed.12826>.
- Vadillo, I., Benavente, J., Carrasco, F., Soler, A., Liñán, C., 2010. Isotopic (13C) signature of CO₂ sources in the vadose zone of a Mediterranean karst (Nerja cave site, southern Spain). In: Andreo, B., Carrasco, F., Durán, J.J., LaMoreaux, J.W. (Eds.), *Advances in Research in Karst Media*. Springer, Berlin, Heidelberg, pp. 463–468.
- Vieten, R., Winter, A., Samson, A., Cooper, J., Wrapson, L., Kambesis, P., Lace, M., Nieves, M., 2016. Quantifying the impact of human visitation in two cave chambers on Mona Island (Puerto Rico): implications for archaeological site conservation. *Cave Karst Sci.* 43, 79–85.
- White, W.B., 1988. *Geomorphology and Hydrology of Karst Terrains*. Oxford University Press, Nueva York 464 pp.
- White, W.B., 1997. Thermodynamic equilibrium, kinetics, activation barriers, and reaction mechanisms for chemical reactions in the Karst Terrains. *Environ. Geol.* 30 (1–2), 46–58.